Journal of Molecular Structure 1225 (2021) 129192

Contents lists available at ScienceDirect

Journal of Molecular Structure

journal homepage: www.elsevier.com/locate/molstr

Design, click conventional and microwave syntheses, DNA binding, docking and anticancer studies of benzotriazole-1,2,3-triazole molecular hybrids with different pharmacophores

Shaya Yahya Alraqa[a], Khalid Alharbi[a], Ateyatallah Aljuhani[a], Nadjet Rezki[a], Mohamed Reda Aouad[a], Imran Ali[a,b,*]

[a] Department of Chemistry, College of Science, Taibah University, Al-Madinah Al-Munawarah 30002, Saudi Arabia
[b] Department of Chemistry, Jamia Millia Islamia (A Central University), New Delhi 110025, India

ARTICLE INFO

Article history:
Received 6 May 2020
Revised 29 August 2020
Accepted 1 September 2020
Available online 2 September 2020

Keywords:
Benzotriazole-1,2,3-triazole
Conventional and microwave synthesis
DNA binding
Docking study
Anticancer activity

ABSTRACT

Despite the availability of some drugs, there is an urgent need for effective anti-cancer medication. It is due to various side effects and non-functionality of the present drugs; especially at the late stage of cancer. Therefore, three series (**4a-e, 6a-e** and **8a-j;** 21 compounds) of benzotriazole-1,2,3-triazole hybrids (carrying different pharmacophores) have been designed and synthesized (by both conventional and microwave syntheses) through the Cu(I)-catalyzed click 1,3-dipolar cycloaddition reaction of the propargylated benzotriazole with the appropriate aliphatic, aromatic and phenyl/benzyl acetamide azides. The syntheses times were from 6 to 12 h and 4 to 8 min in conventional and microwave syntheses. The yields were 80 to 86% and 89 to 95% in conventional and microwave syntheses; confirming microwave synthesis as an economic and eco-friendly method. These compounds were characterized by proper spectroscopic methods. The anticancer activities with A549 and H1299 lung cancer cell lines were in the range of 70.0 to 90.0% for **4a-e** series, 78.0 to 90.0% for **6a-e** series and 81.0 to 90.0% for **8a-j** series. The reported compounds showed good DNA binding constants in the range of 1.3×10^3 to 11.90×10^5 M^{-1}. The docking results suggested strong DNA bindings of the reported compounds in the minor grooves of DNA; through hydrogen bonding and hydrophobic interactions. The quite good anticancer activities and high DNA binding constants have indicated that the reported molecules may be future anticancer agents.

1. Introduction

Cancer is one of the most deadly diseases and the leading cause of a large number of global deaths. As per the World Health Organization (WHO) 2018, the latest estimate is 9.6 million deaths and 18.1 million clinical cases, which are in constant increase; especially in developing countries [1]. Although great efforts have been made in the field of cancer prevention and treatment over the last few decades yet success remains a challenge. Azoles derivatives are one of the crucial structural nitrogen-containing heterocycles, which exhibited numerous biological activities and have attracted considerable attention from medicinal chemists. In particular, the five-membered ring triazoles including 1,2,3-triazole, 1,2,4-triazole and benzofused triazole as well as their derivatives usually have remarkable pharmacological properties such as anticancer [2,3], antifungal [4], antibacterial [5,6] and antiviral [7] activities. It is quite interesting that the 1,2,3-triazoles can form non-covalent interactions like hydrogen bonds, hydrophobic interactions, Van der Waal's forces and dipole-dipole bonds with DNA and other cell biomolecules; altering biological activities [8].

Recently, molecular hybridization is a well-known and effective linking approach in the medicinal chemistry, which consists of the combination of two or more bioactive molecules in a new single chemical framework. It is capable to modulate multiple targets of interest in the development of new synthetic hybrid molecules called drug-like-properties [9,10]. Thus, to address the challenge in this strategy, the selection of the privileged core from linker-to fragment-based hybrids was the critical issue for impacting the synergetic effect of the right target combination compared to the parental compounds [11–16]. Up to date, there are several hybrid molecules, which have been launched to the clinical trials for the conduct of various diseases. Hybridization of 1,2,3-triazole framework with other pharmacophores has become progressively useful and significant in building bioactive and useful molecules [17–19].

* Corresponding author.
E-mail addresses: drimran.chiral@gmail.com, drimran_ali@yahoo.com (I. Ali).

https://doi.org/10.1016/j.molstruc.2020.129192
0022-2860/

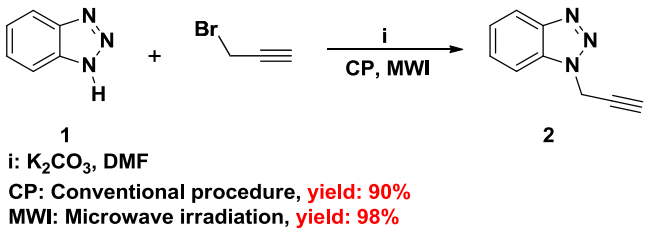

Scheme 1. Propargylation of the benzotriazole 1.

The main efforts in our laboratory have been focused on the development of new methodologies for the syntheses of new heterocyclic hybrid molecules starting from some biologically active functionalized moieties and chiral separation [22–25]. Amongst these, the benzotriazole [20,21] and 1,2,3-triazole derivatives [22–24] were selected as privileged scaffolds for library design and development of targeted drug candidates. Moreover, the presence of several functionalities in their structures becomes a subject of current interest for exalting their biological properties [26]. In this respect, we report herein the hybridization of benzotriazole and 1,2,3-triazoles with several functionalities, including amide, ketone, ester and/or carboxylic acid; *via* click conventional and microwave routes, as a continuation of our previous work on the use of microwave technology in our laboratory [27,28,29,30,31]. These molecules were screened for their anticancer activities on the different cell lines. To determine the anti-cancer mechanism DNA binding and docking studies are also performed. The results reported herein.

2. Results and discussion

2.1. Chemistry

In the present work, the click synthetic methodology has been adopted for the synthesis of a series of novel benzotriazole-1,2,3-triazole hybrids carrying different pharmacophoric center under conventional and microwave circumstances, as illustrated in Schemes 1,2,3,4.

2.1.1. Conventional assisted organic synthesis

The click reaction required first the synthesis of the propargylated benzotriazole **2** *via* base assisted alkylation of benzotriazole (**1**) with propargyl bromide in the attendance of potassium carbonate as base and DMF as solvent (Scheme 1). The reaction required heating 2 hr at 80 °C to afford alkyne derivative **2** in 90% yield.

The structure of compound **2** has been deduced from its spectral data (IR, ^{1}H NMR and ^{13}C NMR), which are in agreement with the literature [32]. The IR spectrum showed the absence of the -NH absorption band and the appearance of two characteristic sharp absorption bands at 2150 and 3300 cm^{-1} credited to the alkyne (-**C≡C-**) and (**≡C–H**) group, respectively. In addition, the ^{1}H NMR spectrum also revealed the disappearance of the benzotriazole -NH proton and the presence of the diagnostic propargyl **≡C–H** and -NC**H**$_2$ protons as two singlets at δ_H 3.61 and 5.74 ppm. The signals belonging to these carbons (-NC**H**$_2$ and -**C≡C-**) resonated at δ_C 37.77, 77.38 and 77.66 ppm, respectively. These results confirmed the incorporation of a propargyl group in the structure of benzotriazole.

The click 1,3-dipolar cycloaddition reaction of benzotriazole-based alkyne **2** with several un/functionalized aromatic azides **3a-e**; catalyzed by copper sulfate and sodium ascorbate in DMSO:H_2O (1:1, v/v) at room temperature for 12 hr; afforded the targeted benzotriazole-1,2,3-triazole molecular conjugates **4a-e** in 80–83% yields (Scheme 2). It should be noted that the aromatic azides **3a-e** were prepared according to the reported procedure [33] *via* diazotization of the respective anilines by sodium nitrite in HCl followed by treatment with sodium azide.

The structures of the click products **4a-e** have been recognized on the basis of their spectroscopic data. In their IR spectra, the absence of the characteristic alkyne absorption bands (-C≡C and ≡C–H) of their precursor **2** established the achievement of the click reaction. The ^{1}H NMR spectra also confirmed the disappearance of the alkyne proton ≡C**–H** and the appearance of a distinct singlet attributable to the 1,2,3-triazole proton at δ_H 9.06–9.19 ppm. Also, the presence of a phenyl ring in the structure of the 1,2,3-triazole **4a-e** at position N-1 was clearly evidenced through the appearance of 3 to 4 additional aromatic protons in the aromatic region. The involvement of the alkyne group in the click reaction was also supported by ^{13}C NMR analysis which exposed the vanishing of the signals assigned to the **-C≡C-** carbons and the appearance of extra aromatic signal carbons.

The synthesis of the benzotriazole-1,2,3-triazole hybrids (carrying un/functionalized alkyl side chain **6a-e)** required first the synthesis of the appropriate alkyl azides **5a-e** through the azidolysis of their alkyl halide analogs with sodium azide in acetone:water (1:1) according to the previous procedure [34]. Then, the click ligation of the azide building block of the freshly prepared alkyl azides **5a-e** with the alkyne group of compound **2**; using the same Cu(I)-catalyzed click synthesis described previously; led to the formation of the benzotriazole-based click products **6a-e** in 83–86% yields (Scheme 3).

The formation of the click products **6a-e** has been shown by ^{1}H NMR analyses through the absence of the terminal hydrogen of the ≡C–**H** group and the presence of a diagnostic singlet in the aromatic region at δ_H 8.21–8.30 ppm typical for the C-5**H** proton of

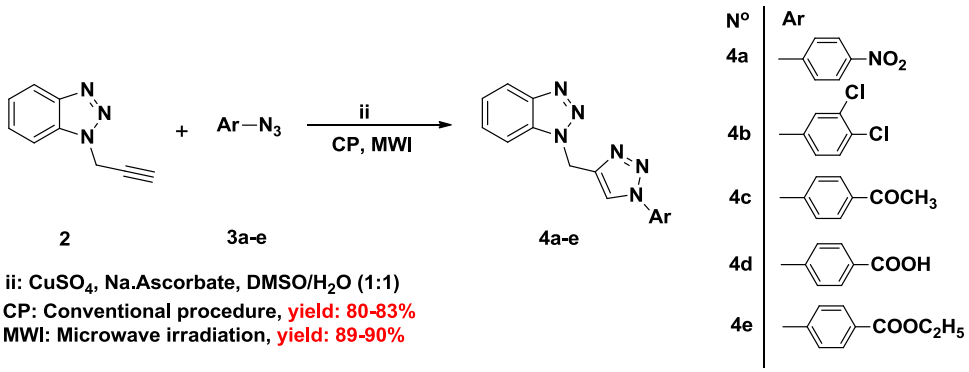

Scheme 2. Click synthesis of benzotriazole-1,2,3-triazole hybrids carrying un/functionalized aromatic side-chain 4a-e.

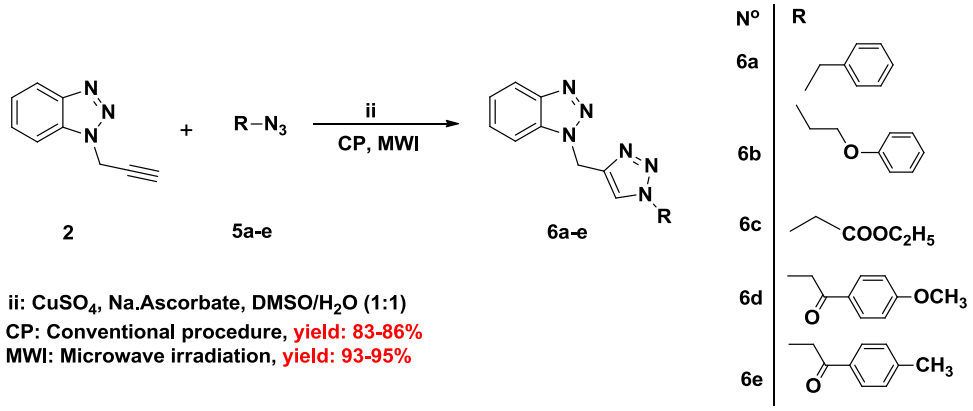

Scheme 3. Click synthesis of benzotriazole-1,2,3-triazole hybrids carrying un/functionalized alkyl side chain 6a-e.

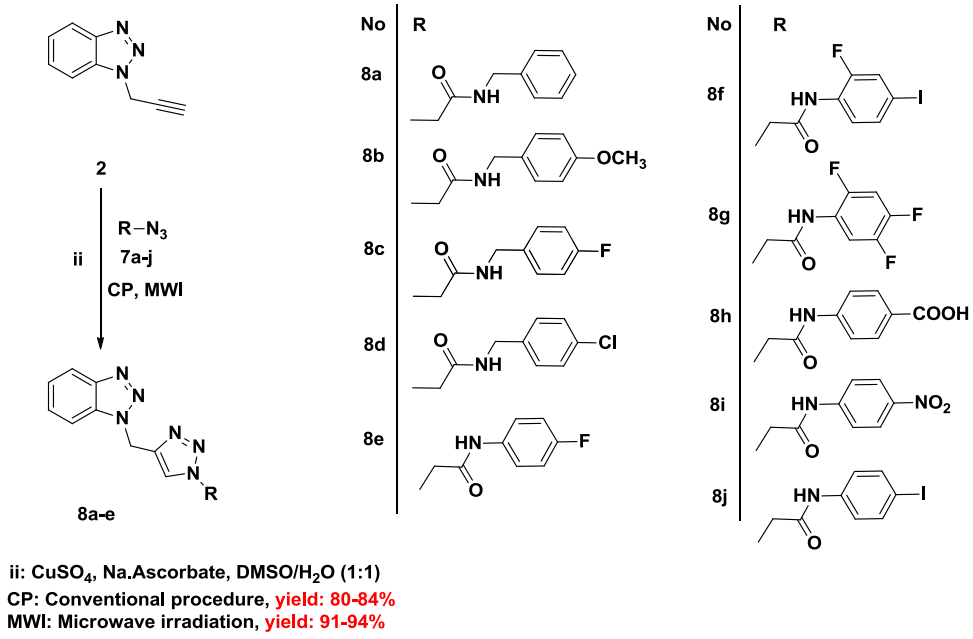

Scheme 4. Click synthesis of benzotriazole-1,2,3-triazole hybrids carrying un/functionalized phenyl and/or benzyl acetamide side-chain 8a-j.

the triazole ring. Besides, the spectra of compounds **6c-e** exposed the attendance of two singlets at δ_H 6.09–6.13 and 5.36–6.14 ppm assigned to the protons bonded to NC**H$_2$** and NC**H$_2$**CO, respectively.

Four extra aromatic protons were also recorded in the aromatic region related to the *p*-substituted phenyl ring for compounds **6d** and **6e**. The success of the click synthesis for the formation of the 1,2,3-triazole scaffold **6a-e** was also confirmed by ^{13}C NMR analysis where the absence of the **-C≡C-** carbons was obvious in their spectra. The spectra also revealed the appearance of new signals at δ_C 56.15–56.31 and 190.76–192.41 ppm, which were attributed, respectively, to the methylene (-**C**H$_2$) and carbonyl (-***C*** = *O*) carbons of the phenacyl side chains in compounds **6d** and **6e**. It should be noted that compound **6a** has been previously reported in the literature with similar proton NMR pattern to that reported in the present manuscript [35].

On the other hand, a series of novel amide based benzotriazole-1,2,3-triazole molecular conjugates **8a-j** have been successfully synthesized in 80–84% yields; under the same optimized Cu(I)-catalyzed click conditions; through the coupling of the propargylated benzotriazole **2** with different phenyl and/or benzyl acetamide azides **7a-j**. The latter was prepared by nucleophilic acylation of the appropriate anilines and/or benzyl amines with chloroacetyl choride followed by azidolysis of the resulting chloroacetamide intermediates with sodium azide [36].

The ^{1}H NMR spectra of all amide-based click products **8a-j** were investigated by the presence of a diagnostic signal in the downfield area at δ_H 8.76–11.09 ppm connected to the amide -N**H** proton. Besides, three to five extra protons were recorded in the aromatic region assignable to the aryl side chain appended to the acetamide linkage. The ^{13}C NMR analysis also evidenced the success of the click reaction *via* the appearance of the characteristic acetamide methylene (-**C**H$_2$) and carbonyl (-***C*** = *O*) carbon at δ_C 52.04–52.78 and 164.31–165.92 ppm, respectively.

2.1.2. Microwave assisted organic synthesis

Microwave-assisted propargylation of benzotriazole (**1**) for 2 min afforded the desired benzotriazole-based alkyne **2** in 98% yield (Table 1). On the other hand, the benzotriazole-1,2,3-triazole hybrids **4a-e, 6a-e** and **8a-j** were prepared in respectable yields (89–95%) when the click reactions were assisted by microwave irradiations for 4–8 min (Table 1).

Table 1
MAOS *versus* conventional synthesis of 1,2,3-triazoles **4a-e, 6a-e** and **8a-j**: times and yields.

Compound No	Conventional procedure (CP)[1]		Microwave procedure (MWI)[2]	
	Time (h)	Yield (%)	Time (min)	Yield (%)
2	2	90	2	98
4a	12	82	8	90
4b	12	81	8	89
4c	12	83	8	90
4d	12	80	8	89
4e	12	81	8	89
6a	6	86	4	95
6b	6	85	4	94
6c	6	86	4	94
6d	8	83	6	93
6e	8	84	6	94
8a	8	83	6	93
8b	8	84	6	94
8c	8	84	6	93
8d	8	82	6	91
8e	10	82	7	91
8f	10	84	7	94
8 g	10	83	7	93
8h	10	80	7	91
8i	10	81	7	92
8j	10	81	7	91

[1] CP: alkyne 2 (1 equiv.), azides3a-e, 5a-e and 7a-j (1 equiv.), copper sulfate (0.4 eq), sodium ascorbate (0.75 eq), DMSO: H2O (1:1), room temperature.
[2] MWI: alkyne 2 (1 equiv.), azides3a-e, 5a-e and 7a-j (1 equiv.), copper sulfate (0.4 eq), sodium ascorbate (0.75 eq), DMSO: H2O (1:1), 300 W, 80 °C.

2.1.3. Comparison of conventional and microwave assisted organic syntheses

A comparison of the click conventional and microwave-assisted syntheses is given in Table 1, which showed clearly that the time required for completion of the reactions in click conventional syntheses were varied from 6 to 12 h while these times in click microwave syntheses were ranged from 4 to 8 min. Besides, the percent yields were from 80 to 86% in click conventional syntheses while the values of yield were varied from 89 to 95%. Therefore, it may be mentioned here that microwave-assisted syntheses of the reported molecules are highly economic saving energy, man-power, costly chemicals and operational simplicity. This microwave-assisted method may be highly useful as an alternative eco-friendly source of energy characterized by a significant reduction in reaction time and improvement of reaction yield, as well as high purity.

2.2. DNA binding study

The UV spectra of Ct-DNA in buffer presented 2 peaks at 280 and 260 nm in the ratio of 1.9:1.0 which showed protein-free nature [37]. The concentration of DNA was estimated by molar absorption coefficient $\varepsilon 260 = 6600$ L mol−1.cm−1 [38]. The equal quantity of DNA was added to both reference and the other solutions for the removal of DNA absorbance. The absorption titration trials were led by variable the amount of DNA with a fixed amount of compounds.

DNA is an important pharmacological target of drugs in several diseases chiefly cancer. There are numerous methods to study DNA and drug interactions but, absorption spectroscopy is a modest and powerful instrument. The absorption spectra of the most active compounds of **4e, 6b** and **8d** are given in **Fig. 1**, whereas the others are stated in the supplementary information. In the absence of Ct-DNA, the compounds showed absorbance in the range of 262–302 nm in tris-buffer at biological pH. With adding of different amounts (1.5×10^{-5}, 1.3×10^{-5} and 1.1×10^{-5}) of Ct-DNA to the fixed amount of compounds (1.6×10^{-4} M), the absorption strength of these compounds showed both hypochromism and hyperchromism and varied from one compound to other. Normally, both hypochromism and hyperchromism are the features detected in spectrophotometric titration of minor molecules with Ct-DNA [39–42]. Hypochromism is usually characterized by non-covalently intercalative bindings of the complexes with DNA [43], while hyperchromism most possibly is related to hydrogen bondings or electrostatic [44]. The compounds showing hyperchromism to DNA are detected in grooves binding cases. The binding coefficients of compounds were intended using Benesi–Hildebrand equation [45]. The compounds 4e and 6b showed hyperchromism while compound 8d showed hypochromism (Fig. 1). It is clear from the spectra that the variation in λ_{max} was from 265 to 266 nm (total change 1 nm) with 86.82% hyperchromism for com-

Table 2
Wavelength shifts, % hypochromism and binding constants of **2, 4a-e, 6a-e** and **8a-j**.

Compound	λ_{max} (free)	λ_{max} (bound to DNA)	Change	%Chromism[a,b]	K_b[c] (M^{-1})
2	212 nm	212 nm	0	0.00[a]	1.3×10^5
4a	216 nm	217 nm	1	37.81[a]	1.57×10^5
4b	214 nm	214 nm	0	46.55[a]	2.6×10^5
4c	267 nm	267 nm	0	59.03[a]	3.33×10^5
4d	261 nm	261 nm	0	4.00[a]	11.9×10^5
4e	265 nm	266 nm	1	86.82[a]	7.0×10^5
6a	212 nm	212 nm	0	36.81 [a]	6.0×10^5
6b	212 nm	214 nm	2	74.44[a]	7.5×10^5
6c	270 nm	273 nm	3	24.95[a]	10.2×10^5
6d	213 nm	212 nm	−1	27.78[a]	2.0×10^5
6e	213 nm	213 nm	0	36.26[a]	5.5×10^5
8a	214 nm	214 nm	0	26.45[b]	3.4×10^5
8b	214 nm	214 nm	0	36.97[a]	1.9×10^5
8c	214 nm	214 nm	0	29.21[a]	2.7×10^5
8d	217 nm	220 nm	3	45.46[b]	3.8×10^5
8e	217 nm	219 nm	2	45.31[a]	4.5×10^5
8f	217 nm	217 nm	0	39.14[a]	4.0×10^5
8 g	215 nm	215 nm	0	47.59[a]	8.6×10^5
8h	275 nm	271 nm	−4	119.34[b]	10.1×10^5
8i	214 nm	215 nm	1	49.58[a]	6.57×10^5
8j	213 nm	213 nm	0	31.51[a]	7.2×10^5

[a] % Hyperchromicity (H%)= $[A_f - A_b)/A_f] \times 100$, where A_f and A_b represent the absorbance of free and bound compounds and.
[b] Hyporchromicity.
[c] Binding constants.

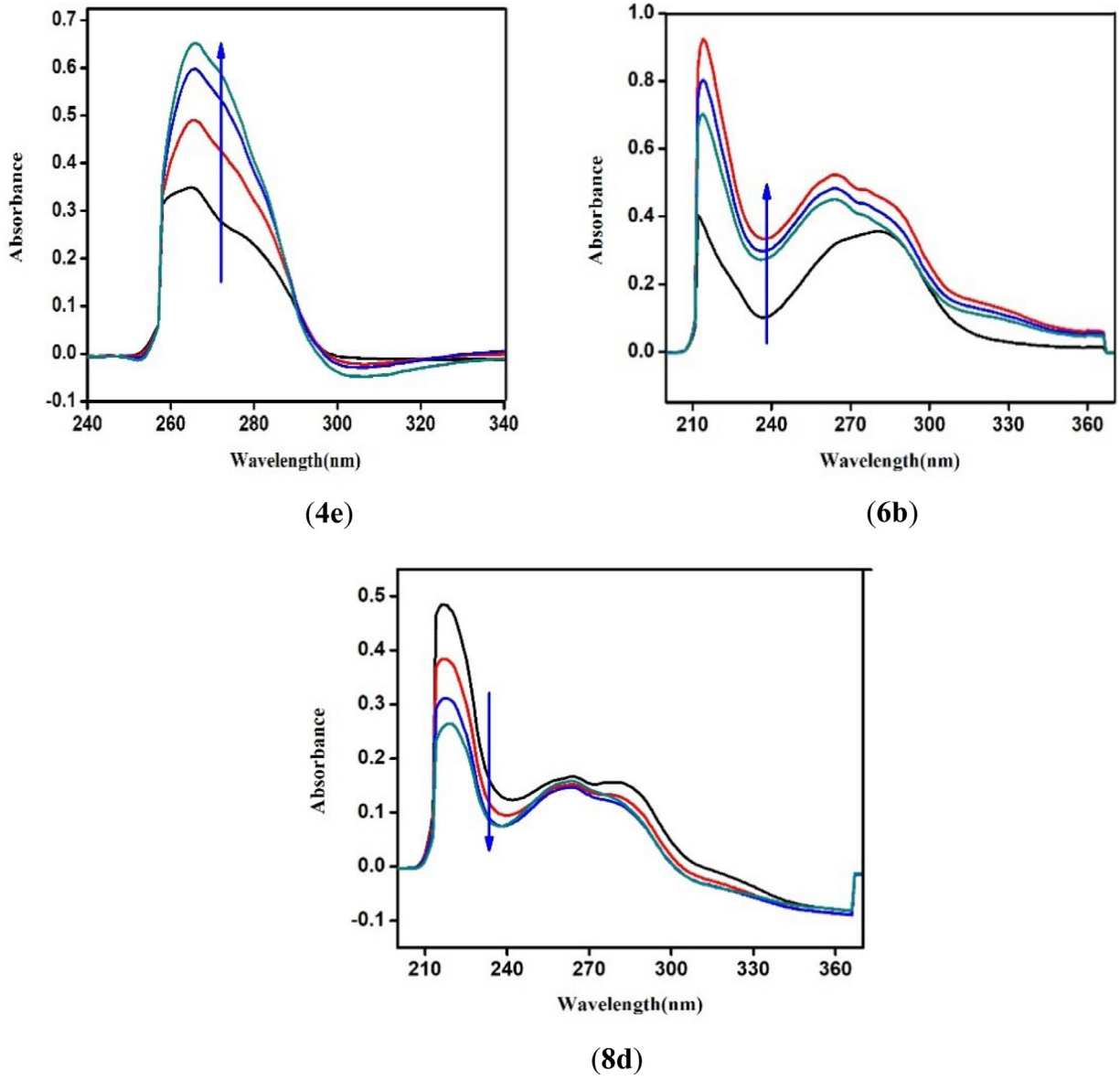

Fig. 1. DNA binding curves for **4e, 6b** and **8d** compounds.

pound 4e. Likewise, for **6b** showed the variation in λ_{max} from 212 to 214 nm (total change 2 nm) with 74.44% hyperchromism. Contrarily, 8d showed hypochromism of 45.46% with changes in λ_{max} from 217 to 220 (total change 3 nm). All these compounds showed bathochromic shifts. These variations showed that these compounds (**4e, 6b** and **8d**) have interacted with Ct-DNA *via* non-covalently intercalations, which could be owing to the stacking interactions between two chromophores. The intrinsic DNA binding coefficients were calculated for all compounds ranging from 1.3×10^3 to 11.90×10^5 M^{-1} (**Table 3**). In addition to these three compounds, the compounds 2, 4a, 4b, 4c, 4d, 6a, 6c, 6d, 6e, 8b, 8c, 8e, 8f, 8 g, 8i and 8j showed hypochromism while hyperchromism was shown by 8a and 8 h compounds. The hypsochromic shift was shown by 6d and 8 h compounds while the bathocromic shift was shown by 4a, 6b, 6c, 8e, 8i compound. These changes are the signs of the sensible bindings of compounds with DNA. Lastly, high values of K_b confirmed that the compounds have a good attraction towards Ct-DNA. It can be said that they showed a slight effect in the case of binding with DNA. These can be measured as non-covalent binders [46,47,48,49].

2.3. Anticancer study

In vitro% inhibitions of A549 and H-1229 lung cancerous cells were determined at 50, 100, 200, 300 and 400 µg/mL amounts of the compounds. The outcomes are given in Figs. 2 and 3 (% viability). Initially, the molecules were dissolved in 0.1% DMSO and the cells with DMSO were applied as vehicle controllers. Then, the growth of the molecules was delayed until the control cells touched at the sluggish phase. The cells were counted after 24 hrs. The propagation step for the cells was increased with growing concentrations of the compounds. The results showed the important reticence in cancer cell proliferation. Three series of the compounds *i.e.* **4a-e, 6a-e** and **8a-j** were screened. The activities of the reported compounds were compared with the concentration of 400 µg/mL.

It is clear from Fig. 2 that the percentage viability for 4a-e series was in the range of 16 to 22% (% inhibition 78 to 84%) with A549 cell line with minimum viability by compound 4e (16%). In the series of 6a-e the percentage viability was ranging from 11 to 22% (% inhibition 78 to 89) with A549 cell line with minimum viability by compound 6b (11%). Similarly, the percentage viability in

Table 3
The docking results of the reported compounds.

Compounds No	Binding energy (kcal mol^{-1})	No. of H bonds	Residues involved in H-bonding (*Bond length*)	Hydrophobic interaction
2	−3.6	2	244/B/DC'13/O2::N of -*N*= group (3.5) 016/A/DG'12/N1::N of -*N*= group (3.5)	dt8::C1,C2,C3&C4 dc9:: C3,C5,C6,C8 & N2 dc15::C3&C6
4a	−4.6	1	624/B/DC'15/OP2:: O of -NO_2 group (3.5)	dt8::C2,C3,C12,C6,C10 & N7 dc9:: C2 & C3 dc13:: O2,N3,O1 & C7 dc15::C11, C13 & C15
4b	−4.8	1	263/A/DG'10/O6::N of -*N*= group (3.4)	dt8::C2,C4,C13,C11 & N6 dc9:: C2 & C4 dc13:: C11 & C12 dc15::C12, C14& C15 dg14::C7
4c	−4.7	1	624/B/DG'14/OP2:: N of -*N*= group (3.5)	dt8::C1 & C2 dc9:: C1 & C2 dg10:: C17 dg14::C3,C4,C5,C6,C9 & C10 dc15::C4,C6 & C13
4d	−4.7	1	624/B/DC'15/OP2:: O of -NO_2 group (3.3)	dt8::C1 & C2 dc9:: C1,C2 & C7 dg14:: C3,C4,C5,C6,C9,C10 & C12 dc15::C12 dg10::C15
4e	−4.4	1	624/B/DC'15/OP2:: O of -COO- group (3.3)	dt8::C8,N2 & N3 dc9:: N2 & C17 dg10:: C13 dc15::C5,C6,C9,C10,C11,C13& C18 dg14:: C3,C5,C9,C16 & C18
6a	−4.5	2	127/A/DC'9/N4::N of -*N*= group (3.5) .127/B/DC'15/N4::N of -*N*= group (3.6)	dt8::N3 dc13:: C3,C8 & C1 dg10:: C15 dc15::C4,C10,C11,C12 & C13 dg14:: C15
6b	−4.8	2	127/B/DC'15/N4::N of -*N*= group (3.6) .624/B/DG'14/OP2::O of -O- group (3.3)	dt8::C1 &C3 dc9:: C2,C3 & C6 dg10:: C17 & C11 dc15::C3,C4,C5,C9,C12 & C17 dg14:: C12,C15 & C17 dg16::C1
6c	−4.1	1	624/B/DC'15/OP2:: O of -COO- group (3.5)	dt8::C1,C2,C3&C4 dc9:: C4 & N3 dg10:: C5 dc15::C9 dg13:: C10 & O2 dg14::C5,C10 & N2
6d	−4.5	1	263/A/DG'10/O6::N of -*N*= group (3.6)	dt8::C3,C17,C18 & O1 dc9:: C12,C17 & N5 dg10:: C12,C14 & C15 dc15::C7,C10,C16 & O2 dg14:: C1,C2 & C5
6e	−5.1	1	127/B/DC'15/N4:: O of -CO- group (3.4)	dt8::N2 dc9:: C15,C16 & N15 dg10:: C7 & C15 dc15::C3,C4,C10,C11,C13 & C18 dg14:: C2,C7 & C10 dc13::C1 & C2
8a	−5.1	1	127/B/DC'15/N4:: O of -CONH- group (3.3)	dt8::C5,C10&N3 dg10:: C14 & C16 dc15::C2,C3,C4,C7 & C8 dg14:: C15 & C18
8b	−4.7	1	263/A/DG'10/O6:: H of -CONH- group (2.3)	dt8::N1 & C16 dc9:: C12 dg10:: N7 dc15::C7,C13&N3 dg14:: C1,C2,C8,C10,C15& C17 dc13::C3& C5
8c	−5.4	2	263/A/DG'10/O6:: O of -CONH- group (3.4).263/B/DG'14/O6:: O of -CONH- group (3.5)	dt8::C7 & N13 dg10:: C13 & C16 dc15::C1,C2,C3,C9,C8 & C15 dg14:: C14,C18 & N2

(*continued on next page*)

Table 3 (*continued*)

Compounds No	Binding energy (kcal mol^{-1})	No. of H bonds	Residues involved in H-bonding (*Bond length*)	Hydrophobic interaction
8d	−5.2	2	127/B/DC'15/N4::N of -*N*= group (3.*5*) 624/B/DC'15/OP2::O of -CONH- group (3.*4*)	dt8::C1,N3&C9 dg10:: C16 dc15::C1,C4,C6,C7 & C10 dg14:: C1,C15,C17 & N2 dg16::C1
8e	−5.0	2	263/A/DG'10/O6::N of -*N*= group (3.*3*) .263/B/DG'14/O6::N of -*N*= group (3.*4*)	dt8::C2 & C8 dc9:: C3 & C8 dg10:: C11,C13&C15 dc15::C4,C5,C7,C8,C11&C16 dg14:: C16 dg16::C8& C14
8f	−4.7	4	263/A/DG'10/O6::N of -*N*= group (3.*5*) 127/A/DC'9/N4::N of -*N*= group (3.*6*) 263/B/DG'14/O6::O of -CONH- group (3.*1*).263/A/DG'10/O6::O of -CONH- group (3.*3*)	dt8::N2 dc9:: C13&C15 dg10::C15,C13&C4 dc15::O dg14::C2,C3,C7 &C8 dc13::C1& C2
8 g	−4.9	1	263/A/DG'10/O6:: O of -CONH- group (3.*2*)	dt8::N2,N6,O & C16 dc9:: C9,N4 dg10:: C3,C11&C15 dc15:: N5 dg14:: C2,C3,C13 & C14 dc13::C1 & C2
8h	−4.8	2	624/B/DG'14/OP2:: O of -NO_2 group (3.*3*).218/B/DC'13/O5′:: O of -NO_2 group (3.*6*)	dt8::N2 dc9:: C14,C15&N4 dg10:: C7,C14&C15 dc15::C12,C18,N5 & O1 dg14:: C2,C3,C4,C6,C7 & C9 dc13::C1,C4 & O2
8i	−5.1	1	127/A/DC'9/N4::N of -*N*= group (3.*4*)	dt8::C1,C6&N2 dc9::N1&N8 dg10:: C15&C11 dc15::C14,C17,O3&N3 dg14:: C4& C9
8j	−5.0	2	263/A/DG'10/O6::N of -*N*= group (3.*4*) 0.127/A/DC'9/N4::N of -*N*= group (3.*5*)	dt8::C1,C8&N3 dc9:: N1,N7&N3 dg10:: C15&C12 dc15::C3 & C9 dg14:: C6,C16 & C17 dc13::C16,C17 & O

No. of hydrogen bond and residues involved were determined by PyMol.
Hydrophobic interactions by Ligplots.

the series of 8a-j ranged from 11 to 19 (% inhibition 81 to 89) with maximum inhibition by compound 8d (11%). A comparison of the percentage viability in H-1229 cell line by the reported compounds is carried out and given in Fig. 3. It is clear from Fig. 3 that the percent viability for 4a-e series was in the range of 10 to 30 (% inhibition 70 to 90) with A549 cell line with maximum inhibition by compound 4e (10%). In the series of 6a-e the percent viability was ranging from 10 to 12 (% inhibition 78 to 90) with H-1229 cell line with maximum inhibition by compound 6b (10%). Similarly, the percent viability in the series of 8a-j ranged from 8 to 25 (% inhibition 75 to 92) with maximum inhibition by compound 8 h (8%).

The above paragraph explains both viability and inhibition of the reported drugs with both A549 and H-1229 cell lines. The maximum percentage inhibitions of **4a-e** series with A549 and H-1229 cell lines were 84.0% (**4e**) and 90.0%, (**4e**). The order of the anticancer activities was **4e > 4d > 4c > 4a > 4b** and **4e > 4d > 4a > 4c > 4b**. High percentage inhibitions of **6a-e** series with A549 and H-1229 cell lines were 89.0% (**6b**) and 90.0% (**6b**). The order of the anticancer activities with these cell lines was **6b > 6c> 6d > 6a> 6e** and **6b > 6d > 6a > 6c > 6e**. The maximum percentage inhibitions of **8a-j** series with A549 and H-1229 cell lines were 89.0% (**8d**) and 92.0% (**8 h**), respectively. The order of the anticancer activities with these cell lines was **8d > 8e> 8 *g*> 8 *h* > 8b> 8f > 8i > 8c> 8j > 8a** and **8 *g* > 8d> 8c> 8i> 8 *h* > 8f > 8e> 8j > 8a > 8b**. All the compounds showed more than 50% inhibition of the cell lines. Furthermore, maximum inhibition was 70.0 to 90.0% for **4a-e** series, 78.0 to 90.0% for **6a-e** series and 81.0 to 90.0% for **8a-j** series of the reported compounds. The percentage reticence was found to be good for **4e, 6b, 8d** and **8 h** compounds and, hence, these compounds may be the imminent molecules for giving cancer.

2.4. Docking study

The efforts were made to determine the interaction mechanism of the reported molecules with DNA by docking study. The different binding energies are given in Table 3. This article describes twenty-one compounds and the binding study was performed with all these compounds. The binding energies of the compounds with DNA ranged from −3.6 to −5.2 kcal/mol because of the different structures of the organic molecules. Also, DNA bond establishment with hydrogen was based on the different structures of the molecules. In these compounds, there were different numbers of hydrogen bonds in the structures. The structures of **4a-e, 6c, 6d, 6e, 8a, 8b, 8 g** and **8i** have one hydrogen bond, while **2, 6a, 6b, 8c, 8d, 8e, 8 h** and **8j** structures formed two hydrogen bonds. One the other hand, **8f** structure formed four hydrogen bonds. Besides, hydrophobic interactions were also different in different structures. Afterward hydrogen bond establishment study, the hydrophobic connections were seen utilizing ligplot software.

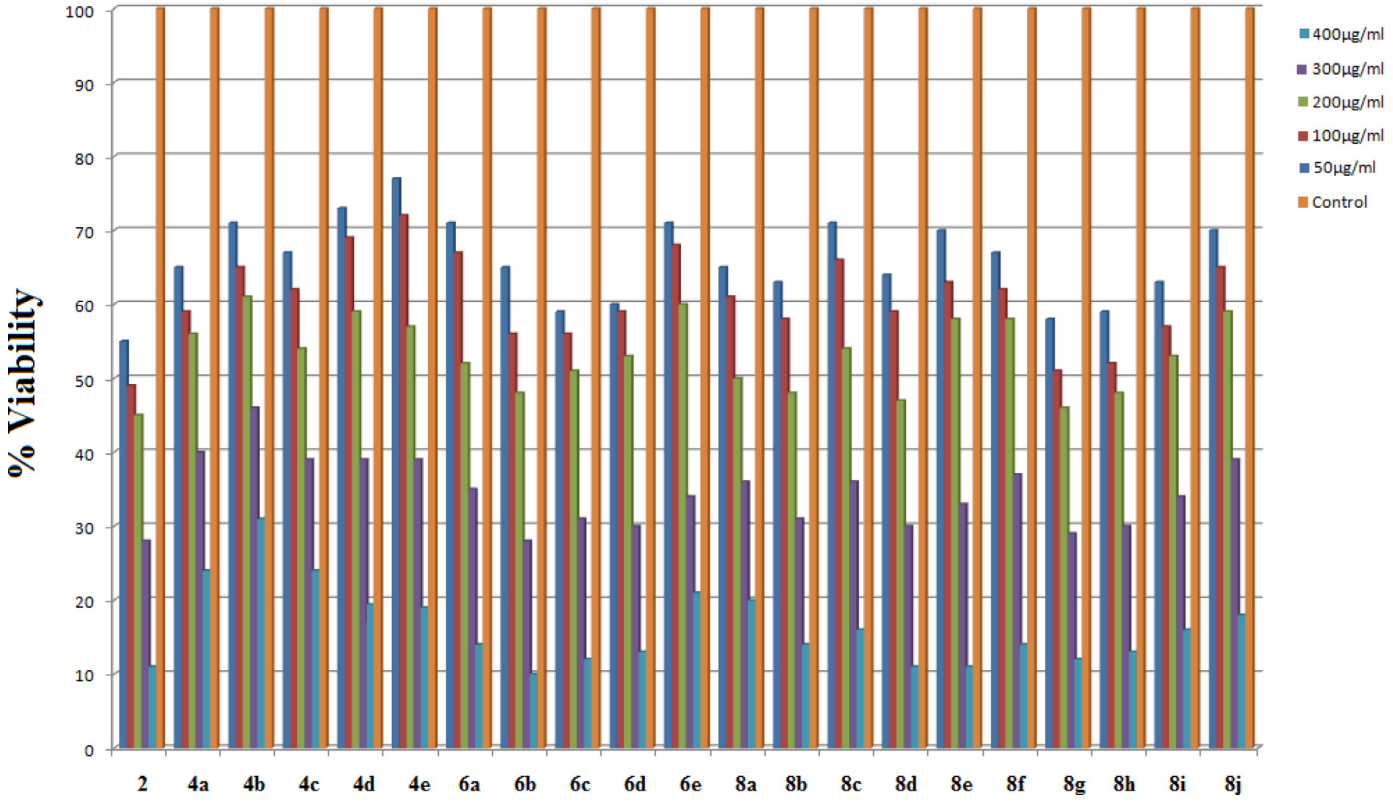

Fig. 2. Anticancer activities of the reported compounds on A549 cell line.

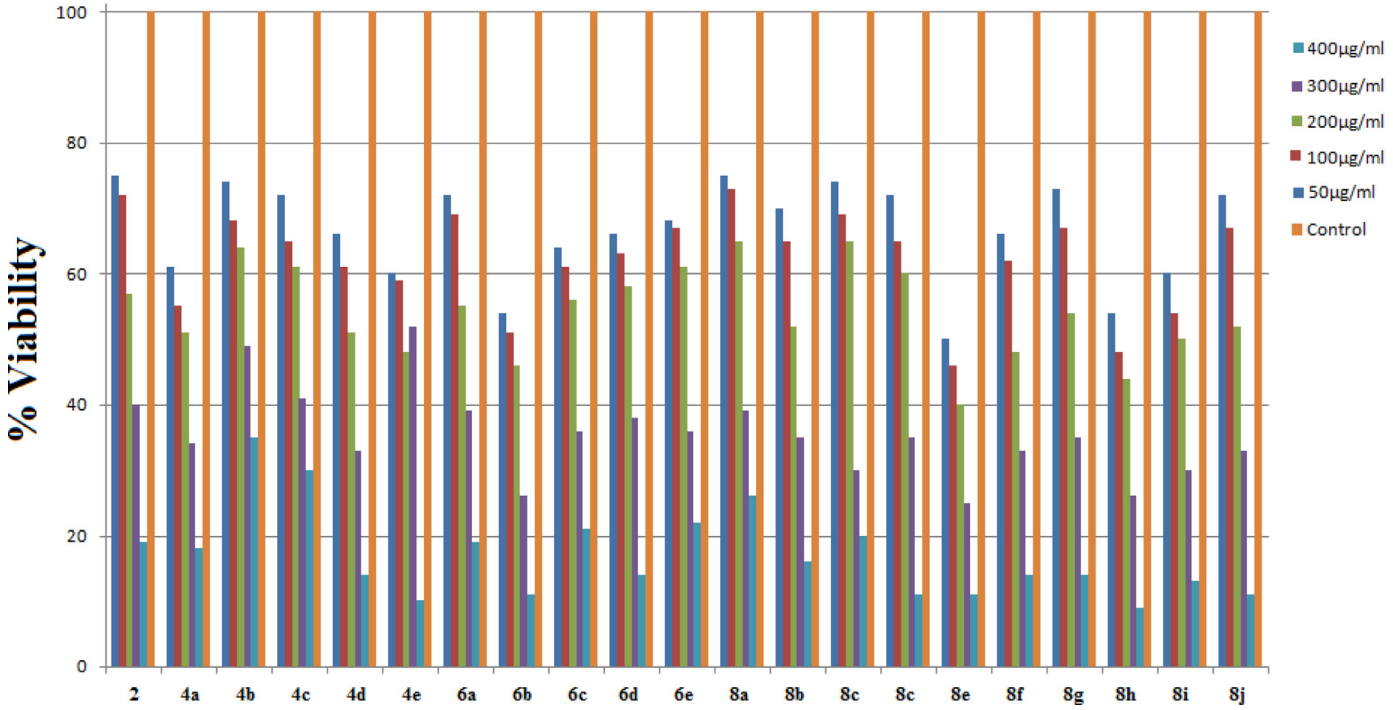

Fig. 3. Anticancer activities of the reported compounds on H1299 cell line.

The collective residues of DNA involved with the reported compounds were dc9, dc13, dc14, dc15, dg10, dg13, dg14, dg16 and dt8. The interactions models of the most active compounds (**4e, 6b** and **8d**) are given in Fig. 4, whereas rests are listed in the supplementary information. It is observed from docking models that all the molecules favored DNA minor grooves for the interactions. It was also seen that all the molecules oriented themselves in such a fashion that their active sites were inside the minor grooves. The results of DNA binding study were in good agreement with those of the docking study. It is very significant to observe that all the molecules showed different docking results; confirming their different anticancer activities.

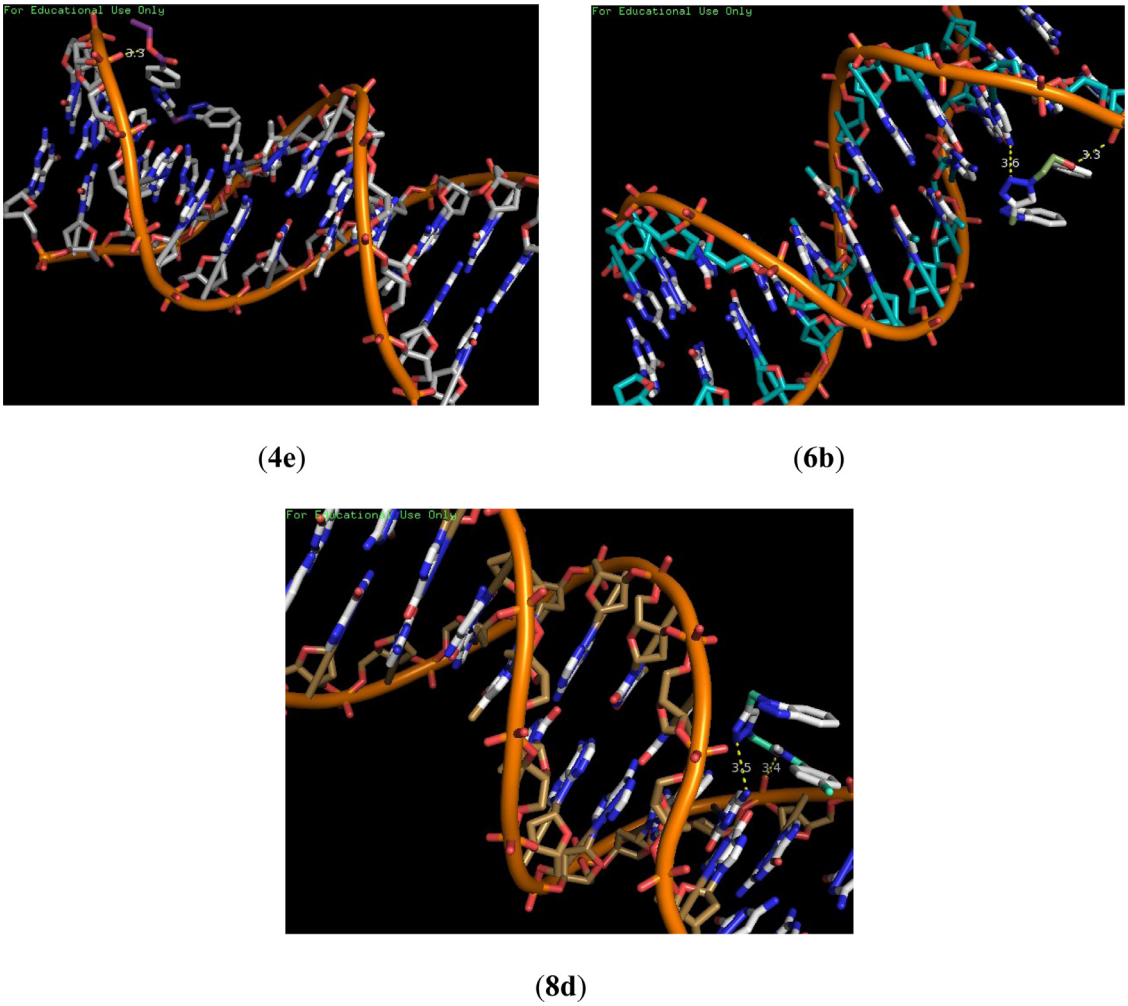

Fig. 4. The docking models of **4e, 6b** and **8d** compounds.

3. Conclusion

Newer series of benzotriazole-1,2,3-triazole hybrids carrying different pharmacophores **4a-e, 6a-e** and **8a-j** were designed and prepared. The yields were 80 to 87% in click conventional syntheses while the values of yields were varied from 89 to 96% in microwave synthesis. The time required for the completion of the reactions in click conventional syntheses were varied from 6 to 20 h while these times in click microwave syntheses were ranged from 2 to 8 min. Besides, the percent yields were from 80 to 87% in click conventional syntheses while the values of yields were varied from 89 to 96%. Therefore, it is concluded that the microwave-assisted synthesis of the reported molecules is highly economic saving energy, man-power and costly chemicals. These microwave-assisted methods may be the choice for the industries. Presently, the world is running under strong economic pressure and under such situations, the reported procedures may be highly useful for the production of the reported molecules at the industrial level. The reported compounds showed good DNA binding constants in the range of 1.3×10^3 to 11.90×10^5 M^{-1}. The anticancer activities were in the range of 86.0 to 90.0% for **4a-e**, 89.0 to 90.0% for **6a-e** series and 89.0 to 90.0% for **8a-j** series. The docking results suggested strong DNA bindings of the reported compounds in minor grooves of DNA; through hydrogen bondings and hydrophobic interactions. These results indicated that the reported compounds may be used as promising anti-cancer drugs.

4. Experimental section

4.1. Synthesis and characterization of 1-(prop–2-yn-1-yl)–1H-benzo[d][1,2,3]triazole (2)

Conventional procedure: To a mixture of benzotriazole (**1**) (10 mmol), potassium carbonate (11 mmol) and DMF (20 ml) were added with stirring propargyl bromide (12 mmol). The mixture was stirred at 80 °C for 2 h until the intake of the starting material exhausted; as indicated by TLC (hexane-ethyl acetate). The reaction mixture was poured into crushed ice and the resulting solid was composed and recrystallized from ethanol to afford the targeted propargylated benzotriazole **2** as colorless crystals in 90% yield, mp: 55–56 °C (Lit. mp: 57–58 °C [50]). IR (υ, cm^{-1}): 1570 (C = C), 2150 (C≡C), 2930 (C–H al), 3040 (C–H ar), 3300 (≡CH). ^{1}H NMR (400 MHz, DMSO–d_6): δ_H 3.61 (s, 1H, ≡CH), 5.74 (s, 2H, NC**H**$_2$), 7.45 (t, 1H, J = 8.0 Hz, Ar-**H**), 7.61 (t, 1H, J = 8.0 Hz, Ar-**H**), 7.93 (d, 1H, J = 8.0 Hz, Ar-**H**), 8.10 (d, 1H, J = 8.0 Hz, Ar-**H**). ^{13}C NMR (100 MHz, DMSO–d_6): δ_C 37.77 (N**C**H$_2$); 77.38, 77.66 (**C≡C**); 111.12, 119.77, 124.77, 128.15, 132.77, 145.72 (Ar-**C**). The spectral data of compound **2** are in agreement with the literature [32]. Anal. Calcd. for $C_9H_7N_3$: C, 68.78; H, 4.49; N, 26.74. Found: C, 68.61; H, 4.55; N, 26.67.

Microwave procedure: Benzotriazole (**1**) (1 mmol), potassium carbonate (1.1 mmol), propargyl bromide (1.2 mmol) and DMF (5 mL) were kept in locked borosilicate glass container fitted with a silicone cap and open to irradiation for 2 min at 50 °C by means of a microwave reactor at 300 W. The reaction was treated as defined in the conventional process previously given for alkyne **2** (98% yield).

4.2. General click procedure for the synthesis of 1,2,3-triazoles 4a-c, 6a-c and 8a-j

Conventional procedure: A solution of copper sulfate (0.10 g) and sodium ascorbate (0.15 g); in water (10 mL); was added to a solution of alkyne **2** (1 mmol) in DMSO (10 mL) with stirring. Thereafter, an appropriate azide (1 mmol) was added, and the reaction mixture was stirred at room temperature for 4–10 h. The reaction was monitored *via* TLC (hexane-ethyl acetate), and after the completion of the reaction, iced-water was added in the mixture. The precipitate made was collected by filtration, treated with a saturated solution of NH_4Cl and recrystallized from ethanol/DMF to give the targeted 1,2,3-triazoles **4a-c, 6a-c** and **8a-j**.

Microwave procedure: Alkyne **2** (1 mmol), copper sulfate (0.10 g) and sodium ascorbate (0.15 g) in water (10 mL) and an appropriate azide (1 mmol) and DMSO (10 mL) were placed in shut borosilicate glass container fitted with a silicone cap and open to irradiation for 3–8 min using a microwave reactor. The reaction was managed as defined in the conventional procedure outlined earlier to give the same click products **4a-c, 6a-c** and **8a-j**.

The characterization of the compounds is given in supplementary information

4.3. DNA binding study

DNA binding study is one of the significant tools to assess the activities of the newly synthesized molecules. It is because the cancer is directly associated with DNA activities in the body. The reported compounds interactions were determined with Ct-DNA (at pH 7.4) in a solution of distilled water comprising tris-(hydroxymethyl)-amino methane buffer (Tris, 10^{-2} M). Originally, the concentration of newly prepared Ct-DNA solution was determined on UV–Vis absorption spectrophotometry at a wavelength of 260 nm ($\varepsilon = 6600\ M^{-1}cm^{-1}$) by knowing its absorbance [51]. The absorption spectra of newly prepared compounds at a fixed concentration of (1.6×10^{-4} M) were taken separately and then with the different amounts of DNA (1.5×10^{-5}, 1.3×10^{-5} and 1.1×10^{-5}) were added. The λ_{max} was noted and the absorbance of the mixture *i.e.* with each dissimilar solution of DNA and the compounds was also dignified. To produce constant results, the experiments were repeated five times ($n = 5$). The intrinsic DNA binding coefficients (K_b) were resolved by Benesi-Hilderbrand equation (**eq. 4.6**) as by Wolfe et al. [52]. The equation is as follows:

$$[DNA]/(\varepsilon_a - \varepsilon_f) = [DNA]/(\varepsilon_a - \varepsilon_f) + 1/K(\varepsilon_b - \varepsilon_f) \quad (1)$$

Where, absorption coefficients, ε_a, ε_f, and ε_b represents A_{obs}/[*compound*], extinction coefficient for the complex and the extinction coefficient for the complex in the completely bound form. The intrinsic binding coefficients for the dissimilar compounds (K_b) were dogged by the division of slopes and the intercepts of the plots of *[DNA]* / (ε_a - ε_f) *vs [DNA]*.

4.4. Anticancer study

The anti-proliferative activities of the compounds were performed with 2 lung cancer cell lines (A549 and H-1229). These cells were sowed in a 96 well plate and incubated. At around 61–71% confluence, the cells were preserved with concs. (400, 300, 200, 100, and 50, μg/mL) of the reported compounds and permitted to incubate for the next 24 h. The cells were examined by adding 15.0 μL (5.0 mg/mL MTT). At 37 °C for 4 h, the individual medium from each well was cleared. The cells were re-suspended in 100 μL of DMSO and the plate directly covered with aluminum foil, shadowed by mild shaking on a shaker for around 15 min. Absorbance was recorded at 540 nm [45] and the percent stop in proliferation was intended by the formula in Eq. (2).

$$\%\,\text{Inhibition} = \left[\left(A_{Control} - A_{Sample}\right)/A_{Control}\right] \times 100 \quad (2)$$

The detailed procedure is given in Supplementary information.

4.5. Docking study

The docking studies of 1,2,3- triazole complexes were done by Intel® dual CPU (1.86 GHz) with Windows XP operating system. Marwin Sketch software was utilized to draw the structures of 1,2,3- triazole compounds. The structures were cleaned to 3D and saved in PDB file format [53]. After that, the structure of DNA (pdb ID: 1bna) was downloaded from protein data bank. Using AutoDock Tools (ADT) 4.2 the structure of DNA to be docked was prepared by assigning Gastegier charges, merging non-polar hydrogen atoms and saving it in PDBQT file format. Docking was performed with AutoDock 4.2 (Scripps Research Institute, USA) considering all the rotatable bonds of the ligand as rotatable and the receptor as rigid [54]. Using the same tool, an 1,2,3-triazole compounds (as a ligand) were edited to be saved in PDBQT formate. The grid box size of 60 × 80 × 110 A° with 0.375 A° spacing was used. After saving both files in PDBQT formate, vina software was used to get binding energy/affinity between receptor (DNA) and ligand (1,2,3-triazole compounds). After using vina software, the output file was opened in PyMOL to carry out the molecular docking, virtual screening and binding site analysis and to get an image of interaction and the bond length of the hydrogen bonds between DNA and 1,2,3- triazole compounds.(Table 2)

Declaration of Competing Interest

The authors declare that they have no known competing financial interests or personal relationships that could have appeared to influence the work reported in this paper. The authors declare the following financial interests/personal relationships which may be considered as potential competing interests: Design, click conventional and microwave syntheses, DNA binding, docking and anticancer studies of benzotriazole-1,2,3-triazole molecular hybrids with different pharmacophores

Supplementary materials

Supplementary material associated with this article can be found, in the online version, at doi:10.1016/j.molstruc.2020.129192.

CRediT authorship contribution statement

Shaya Yahya Alraqa: Conceptualization, Methodology. **Khalid Alharbi:** Methodology, Data curation. **Ateyatallah Aljuhani:** Methodology, Software. **Nadjet Rezki:** Software. **Mohamed Reda Aouad:** Methodology, Writing - original draft. **Imran Ali:** Methodology, Writing - review & editing.

References

[1] F. Bray, J. Ferlay, I. Soerjomataram, R.L. Siegel, L.A. Torre, A. Jemal, Global cancer statistics 2018: GLOBOCAN estimates of incidence and mortality worldwide for 36 cancers in 185 countries, CA Cancer J. Clin. 68 (6) (2018) 394–424.
[2] D. Dheer, V. Singh, R. Shankar, Medicinal attributes of 1,2,3-triazoles: current developments, Bioorg. Chem. 71 (2017) 30–54.

[3] Nadjet Rezki, Amjad M. Al-Yahyawi, Sanaa K. Bardaweel, Fawzia F. Al-Blewi, Mohamed R. Aouad, Synthesis of novel 2,5-disubstituted-1,3,4-thiadiazoles clubbed 1,2,4-triazole, 1,3,4-thiadiazole, 1,3,4-oxadiazole and/or Schiff base as potential antimicrobial and antiproliferative agents, Molecules, 20, 2015, 16048–16067.

[4] P. Xin-Mei, C. Gui-Xin, Z. Cheng-He, Recent developments in azole compounds as antibacterial and antifungal agents, Curr. Top. Med. Chem. 13 (16) (2013) 1963–2010.

[5] R. Kaushik, M. Chaud, S.C. Jain, Synthesis and antibacterial evaluation of nitrogen containing novel heterocyclic chalcones, Synth. Comm. 48 (11) (2018) 1308–1315.

[6] M.R. Aouad, M.M. Mayab, A. Naqvi, S.K. Bardaweel, F.F. Al-blewi, M. Messali, N. Rezki, Design, synthesis, in-silico and in-vitro antimicrobial screenings of novel 1,2,4-triazoles carrying 1,2,3-triazole scaffold with lipophilic side chain tether, Chem. Cent. J. 11 (2017) 117–129.

[7] D.J. Zhang, W.F. Sun, Z.J. Zhong, R. Me. Gao, H. Yi, Y.H. Li, Z.G. Peng, Z.R. Li, Synthesis and broad-spectrum antiviral activity of some novel benzo-heterocyclic amine compounds,, Molecules 19 (2014) 925–939.

[8] A. Lauria, R. Delisi, F. Mingoia, A. Terenzi, A. Martorana, G. Barone, A.M. Almerico, 1,2,3-Triazole in heterocyclic compounds, endowed with biological activity, through 1,3-dipolar cycloadditions, Eur. J. Org. Chem. 2014 (2014) 3289–3306.

[9] C. Viegas-Junior, A. Danuello, V.S. Bolzani, E.J. Barreiro, C.A.M. Fraga, Molecular hybridization: a useful tool in the design of new drug prototypes, Curr. Med. Chem. 14 (2007) 1829–1852.

[10] G. Bérubé, An overview of molecular hybrids in drug discovery, Expert Opin. Drug Discov. 11 (2016) 281–305.

[11] N. Rezki, A Green ultrasound synthesis, characterization and antibacterial evaluation of 1,4-disubstituted 1,2,3-triazoles tethering bioactive benzothiazole nucleus, Molecules 21 (2016) 505–517.

[12] N. Rezki, M.R. Aouad, Green ultrasound-assisted three-component click synthesis of novel 1H-1,2,3-triazole carrying benzothiazoles and fluorinated-1,2,4-triazole conjugates and their antimicrobial evaluation, Acta Pharmaceutica 67 (2017) 309–324.

[13] M.R. Aouad, M.A. Soliman, M.O. Alharbi, S.K. Bardaweel, P.K. Sahu, A.A. Ali, M. Messali, N. Rezki, Y.A. Al-Soud, Design, synthesis and anticancer screening of novel benzothiazole-piperazine-1,2,3-triazole hybrids, Molecules 23 (2018) 2788–2801.

[14] M.R. Aouad, M.A. Almehmadi, N. Rezki, F. Faleh Al-blewi, M. Messali, I. Ali, Design, click synthesis, anticancer screening and docking studies of novel benzothiazole-1,2,3-triazoles appended with some bioactive benzofused heterocycles, J. Mol. Struct. 1188 (2019) 153–164.

[15] I. Ali, Nano anti-cancer drugs: pros and cons and future perspectives, Curr. Cancer Drug Targets 11 (2011) 131–134.

[16] I. Ali, M.N. Lone, Z.A. Al-Othman, A. Al-Warthan, Heterocyclic scaffolds: centrality in anticancer drug development, Curr. Drug Target 16 (2015) 711–734.

[17] Z. Xu, S.J. Zhao, Y. Liu, 1,2,3-Triazole-containing hybrids as potential anticancer agents: current developments, action mechanisms and structure-activity relationships, Eur. J. Med. Chem. 183 (2019) 111700–111737.

[18] K. Bozorov, J. Zhao, H.A. Aisa, 1,2,3-Triazole-containing hybrids as leads in medicinal chemistry: a recent overview, Bioorg. Med, Chem 27 (16) (2019) 3511–3531.

[19] M.E. Welsch, S.A. Snyder, B.R. Stockwell, Privileged scaffolds for library design and drug discovery, Curr. Opin. Chem. Biol. 14 (2010) 347–361.

[20] S. Briguglio, P. Piras, E. Corona, M. Gavini, G. Nieddu, A. Boatto, Carta, Benzotriazole: an overview on its versatile biological behavior, Eur. J. Med. Chem. 97 (2015) 612–648.

[21] B.V. Suma, N.N. Natesh, V. Madhavan, Benzotriazole in medicinal chemistry: an overview, J. Chem. Pharm. Res. 3 (6) (2011) 375–381.

[22] E. Bonandi, M.S. Christodoulou, G. Fumagalli, D. Perdicchia, G. Rastelli, D. Passarella, The 1,2,3-triazole ring as a bioisostere in medicinal chemistry, Drug Discov. Today 22 (10) (2017) 1572–1581.

[23] Z. Xu, S.–J. Zhao, Y. Liu, 1,2,3-Triazole-containing hybrids as potential anticancer agents: current developments, action mechanisms and structure-activity relationships, Eur. J. Med. Chem. 183 (2019) 111700.

[24] R. Kharb, P. Chander Sharma, M. Sh, Yar, Pharmacological significance of triazole scaffold, J, Enzy. Inhib. Med. Chem. 26 (1) (2011) 1–21.

[25] H.Y. Abou-Enein, I. Ali, 25 newHPLC enantiomeric resolution of nebivolol on normal and reversed amylose based chiral phases, Pharmazie 56 (3) (2001) 214–216.

[26] D. Dheer, V. Singh, R. Shankar, Medicinal attributes of 1,2,3-triazoles: current developments, Bioorg. Chem. 71 (2017) 30–54.

[27] N. Rezki, M.R. Aouad, M. Messali, E.S.H. El Ashry, Regioselective (2,3-epoxy)propylation of 5-(3-chlorobenzo[*b*]thien-2-yl)-4H-1,2,4-triazole-3-thione and synthesis of triazolo[2,1-*b*]thiazine analogs under conventional and microwave irradiation, Lett. Org. Chem. 12 (6) (2015) 418–423.

[28] N. Rezki, Green microwave synthesis and antimicrobial evaluation of novel triazoles, Org. Prep. Proced. Int. 49 (2017) 525–541.

[29] A. Aljuhani, W.S. El-Sayed, P.K. Sahu, N. Rezki, M.R. Aouad, R. Salghi, M. Messali, Microwave-assisted synthesis of novel imidazolium, pyridinium and pyridazinium-based ionic liquids and/or salts and prediction of physico-chemical properties for their toxicity and antibacterial activity, J. Mol. Liq. 249 (2018) 747–753.

[30] A.H. Albalawi, W.S. El-Sayed, A. Aljuhani, S.M. Almutairi, N. Rezki, M.R. Aouad, M. Messali, Microwave-assisted synthesis of some potential bioactive imidazolium-based room temperature ionic liquids, Molecules, 23, 2018, 1727–1741.

[31] A. Aljuhani, M.R. Aouad, N. Rezki, O.A. Aljaldy, S.A. Al-Sodies, M Messali, I. Ali, Novel pyridinium based ionic liquids with amide tethers: microwave assisted synthesis, molecular docking and anticancer studies, J. Mol. Liq. 285 (2019) 790–802.

[32] L.A. Perego, R. Blieck, J. Michel, I. Ciofini, L. Grimaud, M. Taillefer, F. Monnierc, Copper-Catalyzed Hydroamination of N-Allenylazoles: access to Amino-Substituted N-Vinylazoles, Adv. Synth. Catal. 359 (2017) 4388–4392.

[33] M.J. Minvielle, C.A. Bunders, C. Melander, Indole-triazole conjugates are selective inhibitors and inducers of bacterial biofilms, Med. Chem. Comm. 6 (2013) 916–919.

[34] N. Devender, S. Gunjan, R. Tripathi, R.P. Tripathi, Synthesis and antiplasmodial activity of novel indoleamide derivatives bearing sulfonamide and triazole pharmacophores, Eur. J. Med. Chem. 131 (2017) 171–184.

[35] O.N. Verkhozina, V.N. Kizhnyaev, L.I. Vereshchagin, A.V. Rokhin, A.I. Smirnov, Synthesis of Polynuclear Nonfused Azoles, Russ. J. Org. Chem. 39 (12) (2003) 1792–1796.

[36] G. Wang, Z. Peng, J. Wang, X. Li, J. Li, Synthesis, *in vitro* evaluation and molecular docking studies of novel triazine-triazole derivatives as potential α-glucosidase inhibitors, Eur. J. Med. Chem. 125 (2017) 423–429.

[37] J. Marmur, A procedure for the isolation of deoxyribonucleic acid from microorganisms, J. Mol. Biol. 3 (1961) 208–218.

[38] I. Ali, M. Nadeem Lone, Z.A. Al-Othman, A. Al-Warthan, Insights into the pharmacology of new heterocycles embedded with oxopyrrolidine rings: DNA binding, molecular docking, and anticancer Studies, J. Mol. Liq. 234 (2017) 391–402.

[39] K. Saleem, W.A. Wani, A. Haque, M.N. Lone, M.-F. Hsieh, I. Ali, Synthesis, DNA binding, hemolysis, and anticancer profiles of copper (II), nickel(II) and iron(III) complexes of a pyrazoline based ligand, Fut. Med. Chem. 5 (2013) 135–146.

[40] I. Ali, M.N. Lone, M.-F. Hsieh, N-Substituted (Substituted-5-Benzylidine) Thiazolidine-2,4-Diones: crystal structure, In silico, DNA binding, and anticancer studies, Biointerface Res. Appl. Chem. 6 (2016) 1356–1379.

[41] I. Ali, W.A. Wani, K. Saleem, M.F. Hseih, Design and synthesis of thalidomide based dithiocarbamate Cu(II), Ni(II) and Ru(III) complexes as anticancer agents, Polyhedron 56 (2013) 134–143.

[42] I. Ali, K. Saleem, D. Wesselinova, A. Haque, Synthesis, DNA binding, hemolytic and anticancer assays of curcumin I based ligands and their ruthenium (III) complexes, Med. Chem. Res. 22 (2013) 1386–1398.

[43] S. Chandrasekaran, Y. Sameena, I.V.M.V. Enoch, Modulation of the interaction of coumarin 7 with DNA by β-cyclodextrin, J. Incl. Phenom. Macrocycl. Chem. 81 (2015) 225–236.

[44] I. Ali, W.A. Wani, A. Khan, A. Haque, A. Ahmad, K. Saleem, N. Manzoor, Synthesis and synergistic antifungal activities of a pyrazoline based ligand and its Copper (II) and Nickel (II) complexes with conventional antifungals, Microb. Pathogen. 53 (2012) 66–73.

[45] X. Shui, M.E. Peek, L.A. Lipscomb, Q. Gao, C. Ogata, B.P. Roques, C.G. Jaureguiberry, A.P. Wilkinson, L.D. Williams, Effects of cationic charge on three-dimensional structures of intercalative complexes structure of a bis-intercalated DNA complex solved by MAD phasing, Curr. Med. Chem. 7 (2000) 59–71.

[46] M.J. Waring, C. Bailly, The purine 2-amino group as a critical recognition element for binding of small molecules to DNA, Gene 149 (1994) 69–79.

[47] C. Rehn, U. Pindur, Molecular modeling of intercalation complexes of antitumor active 9-aminoacridine and a [d,e]-anellatedisoquinoline derivative with base paired deoxytetranucleotides, Monatsh. Chem. 127 (1996) 645–658.

[48] M. Baginski, F. Fogolari, J.M. Briggs, Electrostatic and non-electrostatic contributions to the binding free energies of anthracycline antibiotics to DNA, J. Mol. Biol. 274 (1997) 253–267.

[49] I. Ali, M.N. Lone, H.Y. Aboul-Enein, Imidazoles as potential anticancer agents, Med. Chem. Commun. 8 (2017) 1742–1773.

[50] A. Khalafi-Nezhada, A. Zareb, A. Parhamia, M.N. Soltani Rad, G.R. Nejabat, Highly Regioselective *N*-Alkylation of Benzotriazole under Solvent-Free Conditions, J. Iran. Chem. Soc. 4 (3) (2007) 271–278.

[51] N. Ataci, E. Ozcelik, N. Arsu, Spectrophotometric study on binding of 2-thioxanthone acetic acid with ct-DNA, Spectrochimica Acta Part A: mol, Biomol. Spectr. 204 (2018) 281–286.

[52] A. Wolfe, G.H. Shimer Jr., T. Meehan, Polycyclic aromatic hydrocarbons physically intercalate into duplex regions of denatured DNA, Biochem. 26 (1987) 6392–6396.

[53] M.F. Sanner, Python: a programming language for software integration and development, J. Mol. Graph. Model. 17 (1999) 57–61.

[54] G.M. Morris, D.S. Goodsell, R.S. Halliday, R. Huey, W.E. Hart, R.K. Belew, A.J. Olson, Automated docking using a lamarckian genetic algorithm and and empirical binding free energy function, J. Comput. Chem. 19 (1998) 1639–1662.